

# Quantum teleportation of a squeezed state

N. Takei,<sup>1</sup> T. Aoki,<sup>1,2</sup> S. Koike,<sup>1</sup> K. Yoshino,<sup>1</sup> K. Wakui,<sup>1</sup> H. Yonezawa,<sup>1</sup> T. Hiraoka,<sup>1</sup>  
J. Mizuno,<sup>2,3,4</sup> M. Takeoka,<sup>2,3,4</sup> M. Ban,<sup>2,5</sup> and A. Furusawa<sup>1,2</sup>

<sup>1</sup>Department of Applied Physics, School of Engineering,

The University of Tokyo, 7-3-1 Hongo, Bunkyo-ku, Tokyo 113-8656, Japan

<sup>2</sup>CREST, Japan Science and Technology (JST) Agency, 1-1-9 Yaesu, Chuo-ku, Tokyo 103-0028, Japan

<sup>3</sup>Communications Research Laboratory, 4-2-1 Nukui-Kitamachi, Koganei, Tokyo 184-8795, Japan

<sup>4</sup>CREST, JST, 3-13-11 Shibuya, Shibuya-ku, Tokyo 150-0002, Japan

<sup>5</sup>Advanced Research Laboratory, Hitachi Ltd, 2520 Akanuma, Hatoyama, Saitama 350-0395, Japan  
(Dated: December 24, 2018)

Quantum teleportation of a squeezed state is demonstrated experimentally. We observe the less variance of the teleported squeezed state than that for the vacuum state input. We verify that the teleportation process operates properly for the nonclassical state input. Using fidelity, we evaluate our results. The fidelity for the squeezed state input is  $0.85 \pm 0.05$  which is higher than the classical case of  $0.73 \pm 0.05$ . This work is an important step toward entanglement swapping.

PACS numbers: 42.50.Dv, 03.67.Hk, 03.65.Jd

Quantum teleportation is a method of transporting unknown quantum states from one location to another via classical channels with the assistance of quantum entanglement [1]. This quantum entanglement enables reliable transmission of quantum information contained in quantum systems. It is possible to transfer nonclassical features such as quantum entanglement through this technique. Such a transfer of nonclassical features is a remarkable capacity of quantum teleportation. Therefore this protocol has been playing a central role in quantum communication and computation [2].

Quantum teleportation was originally proposed in discrete variable systems [3]. Experimental demonstrations have been performed on the polarization states of single photon states [3] and on a time-bins state in the telecommunication wavelength [4]. Furthermore quantum teleportation has also been applied to continuous variable systems [5, 6] employing the Einstein-Podolsky-Rosen (EPR) correlation [7]. Experimentally, continuous variable teleportation has been realized for coherent states of optical fields as inputs [8, 9, 10].

However a coherent state does not show nonclassical features. The teleportation protocol is able to transfer arbitrary quantum states and nonclassical features. To verify such a great ability of quantum teleportation, it is desirable to transfer quantum entanglement (entanglement swapping [11]) or the nonclassical states with strong singularities in the Glauber-Sudarshan P-function [12].

In this paper, we demonstrate continuous variable teleportation of a squeezed state. A squeezed state shows a nonclassical feature: the squeezed variance is below the shot noise level. We verify that such a nonclassical feature is preserved in the teleportation process. This work is an important step toward entanglement swapping.

As in the previous works [8, 9, 10], the teleported states in our teleportation experiment are (modulation) sidebands of an optical field. To describe such states, it is convenient to introduce quadrature phase amplitudes  $\hat{x}$  and  $\hat{p}$  corresponding to the real and imaginary part of

an optical field mode's annihilation operator:  $\hat{a} = \hat{x} + i\hat{p}$  (units-free with  $\hbar = 1$ ,  $[\hat{x}, \hat{p}] = i$ ).

Here we consider the teleportation of a "squeezed vacuum" state. For any real experiments, one usually obtains a squeezed vacuum which suffers from some inevitable losses. Such a squeezed vacuum is not a pure but mixed state. This mixed squeezed vacuum can be regarded as a squeezed thermal state. By assuming that  $\hat{x}$  quadrature is squeezed, it can be described by

$$\hat{x}_{\text{in}} = e^{-s} \hat{x}_{\text{in}}^{(\text{th})} \quad \text{and} \quad \hat{p}_{\text{in}} = e^{+s} \hat{p}_{\text{in}}^{(\text{th})}; \quad (1)$$

where  $s$  is the squeezing parameter for an input state and a superscript (th) denotes an initial thermal state. Its variances  $\langle \hat{x}_{\text{in}}^2 \rangle$ ;  $\langle \hat{p}_{\text{in}}^2 \rangle$  become

$$\begin{aligned} \langle \hat{x}_{\text{in}}^2 \rangle &= \hbar \langle \hat{x}_{\text{in}}^{(\text{th})2} \rangle = e^{-2s} \coth(\frac{s}{2}) = 4 \\ \langle \hat{p}_{\text{in}}^2 \rangle &= \hbar \langle \hat{p}_{\text{in}}^{(\text{th})2} \rangle = e^{+2s} \coth(\frac{s}{2}) = 4 \end{aligned}; \quad (2)$$

from the relation of  $\hbar \langle \hat{x}_{\text{in}}^{(\text{th})2} \rangle = \hbar \langle \hat{p}_{\text{in}}^{(\text{th})2} \rangle = \coth(\frac{s}{2}) = 4$ . Here  $\hbar$  is  $1/2k_B T$ ,  $k_B$  is the Boltzmann constant and  $T$  is the temperature. In a broad sense, squeezed thermal states include the state whose squeezed variance is not below the shot noise level (the vacuum variance). In the present work, however, we transport a squeezed state with the squeezed variance less than the vacuum variance (see Fig. 2).

The scheme for the teleportation process is outlined in Fig. 1. First Alice and Bob share the entangled EPR beams, which can be created by mixing two squeezed states at a beam splitter (BS). One of the EPR beams is sent to a sender Alice (mode 1) and the other is to a receiver Bob (mode 2). For the purpose of verifying the protocol, an input state is created by Victor (the "verifier"). Note that an input state is unknown to both Alice and Bob in the ideal case. Alice combines mode 1 and an input state at a 50/50 BS, and then measures  $\hat{x}$  and  $\hat{p}$  quadratures by two homodyne detectors;  $\hat{x}$  for one beam ( $A_x$ ) and  $\hat{p}$  for the other ( $A_p$ ). This measurement corresponds to the Bell-state measurement for continuous

variables[6, 13, 14]. The output photocurrent of classical results are transmitted to Bob through classical channels. Due to the property of the EPR correlations, the effect of Alice's measurement collapses the mode 2 into a state that is very similar to the unknown input state but only differs from it by a phase space displacement. After receiving the classical information from Alice, Bob reconstructs the teleported output state by performing a phase space displacement on the mode 2 beam. His displacement process consists of two parts. One is the amplitude and phase modulations of a light beam based on the classical information from Alice. The other is the coherent combination of this modulated beam and the mode 2 at a highly reflecting mirror (a 99/1 BS in our experiment). In the absence of losses, the variance  $x_{out}$  of  $x$  quadrature associated with the output state is written by [8]

$$x_{out} = g^2 x_{in} + \frac{(1+g)^2}{2} \frac{e^{2r}}{4} + \frac{(1-g)^2}{2} \frac{e^{2r_+}}{4}; \quad (3)$$

where  $g$  is a suitably normalized gain of classical channels and  $r$ ;  $r_+$  are the squeezing and the antisqueezing parameters for squeezed states used to generate the EPR beams. A similar result is obtained for  $p$  quadrature.

When the squeezed state in Eq.(2) is teleported with  $g = 1$ , the teleported state should show the less variance in  $x$  quadrature than that for the case of a vacuum input ( $s = 0$ ;  $r_+ = 1$ ),

$$\begin{aligned} (x_{out})_{sq} &= x_{in} + \frac{2e^{2r}}{4} \\ &< (x_{out})_{vac} = \frac{1 + 2e^{2r}}{4}; \end{aligned} \quad (4)$$

This is because the variance  $x_{in}$  in the present work is less than the vacuum variance  $1/4$ . Although some losses are inevitable and the gain  $g$  might slightly differ from unity in real experiments, the relation of Ineq.(4) would hold fully. We verify that the quantum teleportation process satisfies the above inequality in order to show the preservation of the nonclassical feature during the teleportation process.

Victor analyzes the output from Bob's station and verifies the success of quantum teleportation by using fidelity. When an input state is a mixed state, the fidelity is described as follows[15]:

$$F = \text{Tr} \left[ \rho_{in} \frac{\rho_{out}}{\rho_{in}} \right]^{1/2}; \quad (5)$$

This is an overlap between an input state  $\rho_{in}$  and an output state  $\rho_{out}$ . If an input is a pure state  $j_{in}$ , the fidelity  $F$  becomes  $F = \langle j_{in} | \rho_{out} | j_{in} \rangle$ . In the ideal quantum teleportation, the fidelity goes to unity,  $F = 1$ , whereas  $F = 0$  means that the teleported state is orthogonal to the input state.

Our experimental setup is also shown in Fig.1. We generate three independent squeezed vacuum states. One of

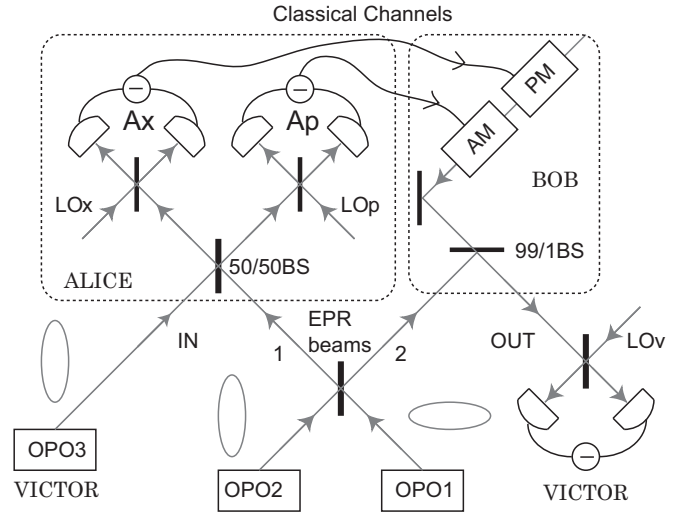


FIG. 1: Schematic setup of the experiment for quantum teleportation of a squeezed state. OPOs represent optical parametric oscillators. AM and PM denote amplitude and phase modulators. LOs are local oscillators for homodyne detection. The ellipses indicate the squeezed quadrature of each beam. All beam splitters except 99/1BS are 50/50 beam splitters.

these states is for an input for teleportation and the other two are used to produce the entangled EPR beams. Each squeezed state is generated by parametric down conversion process in a subthreshold degenerate optical parametric oscillator (OPO) with a potassium niobate crystal temperature tuned and noncritically phase matched. The output of a Ti:Sapphire laser at 860nm is frequency-doubled in an external cavity with the same configuration as the OPOs and divided into three beams to pump the three OPOs. About 3% of the 860nm beam is spatially filtered by a mode cleaning cavity and used for local oscillators (LOs) in homodyne detections and for Bob's displacement beam. Two classical channels are adjusted in a manner described in Ref.[10]. The gains of  $g_x = 0.97 \pm 0.04$ ;  $g_p = 0.97 \pm 0.03$  are obtained for each channels.

The EPR beams are produced by combining two squeezed vacuum states from OPO1 and OPO2 at a 50/50 BS with a  $\pi/2$  phase shift as shown in Fig.1. We characterize the entanglement with the inseparability criterion proposed by Duan et al.[16] and obtain the result  $h[(x_1 - x_2)^2] + h[(p_1 + p_2)^2] = 0.47 \pm 0.04 < 1$ .

We first measure the input squeezed state at the Ap detector at Alice by removing Alice's 50/50 BS. Figure 2 shows the results which are measured by a spectrum analyzer. The minimum noise level is  $-2.66 \pm 0.49$  dB and the maximum noise level is  $7.45 \pm 0.17$  dB compared to the vacuum noise level.

We then proceed to the experiment of teleportation. Alice's measurement results are shown in Fig.3. In the case without the EPR beams as shown in Fig.3(a), a vacuum state invades Alice's 50/50 BS, which causes 50% losses of an input state. As a result, Alice would obtain

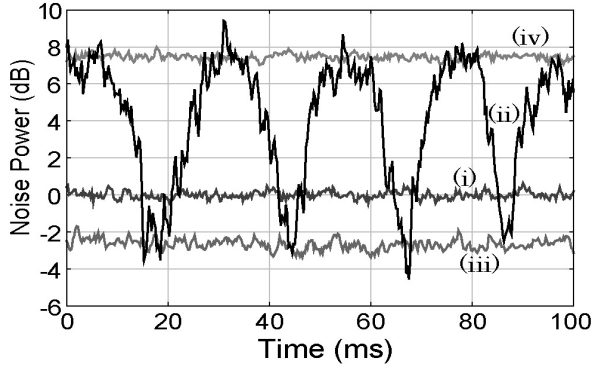


FIG. 2: Noise measurement results on the input squeezed state recorded by the Alice homodyne detector, with Alice's 50/50 BS removed, as a function of time. Trace (i) shows the corresponding vacuum noise level; trace (ii) is the variance of the squeezed state with the LO phase scanned; traces (iii) and (iv) are the minimum and the maximum noise levels with the LO phase locked. The measurement frequency is 1 MHz, resolution bandwidth is 30 kHz, and video bandwidth is 300 Hz. All traces except for (ii) are averaged ten times.

only partial information on the input state. Although the input state is originally squeezed by  $-2.66 \pm 0.49$  dB as in Fig. 2, the observed squeezing at Alice is  $-0.97 \pm 0.28$  dB, which reasonably agrees with the squeezing level with 50% losses. In contrast, when the EPR beam enters Alice's BS, the measured variances are larger than that of the case without the EPR beams as shown in Fig. 3(b). In other words, we put the EPR beam in Alice's 50/50 BS in place of the undesirable vacuum.

Figure 4 shows the Victor's measurement results of the output state from Bob. First we consider the case without EPR beams in Fig. 4(a), which is so-called classical teleportation. In this case, the variances are somewhat large due to the quduty that must be paid for crossing the border between quantum and classical domains [6]. We observe the noise levels of  $4.86 \pm 0.20$  dB and  $4.92 \pm 0.20$  dB in  $\hat{x}$  and  $\hat{p}$  quadratures for the vacuum input. For the squeezed state input, we observe the minimum noise level of  $4.12 \pm 0.23$  dB in  $\hat{x}$  quadrature and the maximum noise level of  $8.92 \pm 0.16$  dB in  $\hat{p}$  quadrature in this classical teleportation.

Next we perform the teleportation with EPR beams as shown in Fig. 4(b) and (c). In the case of a vacuum input, the output variances are reduced from the classical case due to the EPR correlation. We obtain the noise levels of  $2.90 \pm 0.21$  dB and  $3.01 \pm 0.19$  dB in  $\hat{x}$  and  $\hat{p}$  quadratures, respectively.

The squeezed state shown in Fig. 2 is subsequently teleported. We obtain the minimum noise level of  $2.03 \pm 0.24$  dB in  $\hat{x}$  quadrature and the maximum noise level of  $8.18 \pm 0.17$  dB in  $\hat{p}$  quadrature, respectively. The squeezed variance of the teleported state is clearly less than that of the teleported vacuum state in  $\hat{x}$  quadrature, and then the inequality  $(\hat{x}_{\text{out}})_{\text{sq}} < (\hat{x}_{\text{out}})_{\text{vac}}$  is satisfied. Therefore the nonclassical property of squeezing

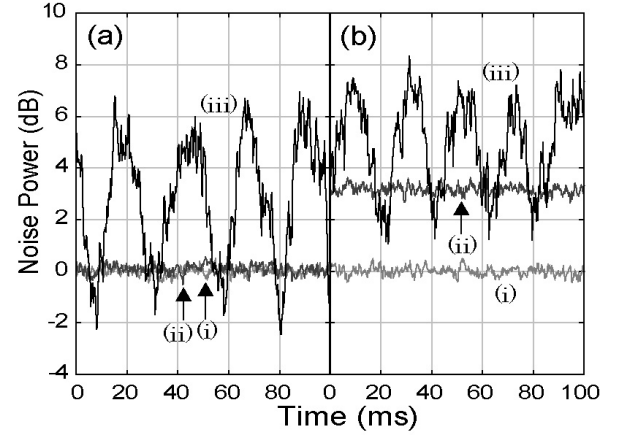


FIG. 3: Noise measurement results on the input states recorded by Alice's Ax homodyne detector. (a) the results for the case without the EPR beam in  $\hat{x}$  quadrature; (b) the results for the case with the EPR beam in  $\hat{x}$  quadrature. In each case, trace (i) represents the corresponding shot noise level; trace (ii) is the variance for the vacuum state input; trace (iii) shows the variance for the squeezed state input with the phase of the input state scanned. In (a), the trace (i) overlaps with the trace (ii). The measurement conditions are the same as for Fig. 2.

is certainly teleported.

We evaluate the success of the teleportation process by fidelity. The teleportation process can be regarded as a generalized thermalizing quantum channel [19] and does not alter the Gaussian character of the input state. Assuming both input and output states show Gaussian distribution, we can characterize these states by measuring the variances of  $\hat{x}$  and  $\hat{p}$  quadratures.

Because a vacuum is one of pure states, the fidelity for the vacuum teleportation is simply given by  $F = 2 / (1 + 4 \langle \hat{x}_{\text{out}}^2 \rangle (1 + 4 \langle \hat{p}_{\text{out}}^2 \rangle))$ . We obtain the fidelity for a vacuum input of  $0.67 \pm 0.02$  with the gain 0.97, which exceeds the classical limit 0.5 [17, 18]. But we do not apply this classical limit to the case of the squeezed state input, since the fidelity depends on an input state like Eq. (5).

It could be considered that a squeezed thermal state input is transformed into another squeezed thermal state in the imperfect teleportation process. For these states, the fidelity in Eq. (5) can be calculated explicitly [20]:

$$F = \frac{2 \sinh(\frac{1}{2}) \sinh(\frac{1}{2})}{\sqrt{Y} - 1};$$

$$Y = \cosh^2(s - s^0) \cosh^2(\frac{1}{2} + \frac{1}{2}) + \sinh^2(s - s^0) \cosh^2(\frac{1}{2} - \frac{1}{2}); \quad (6)$$

Here a superscript  $(^0)$  denotes an output state.

The classical limit has not been discussed for a set of squeezed thermal state inputs so far. We apply the fidelity in Eq. (6) to the particular input state in this experiment. The fidelity for the "perfect" classical teleportation or the classical limit could be inferred from the

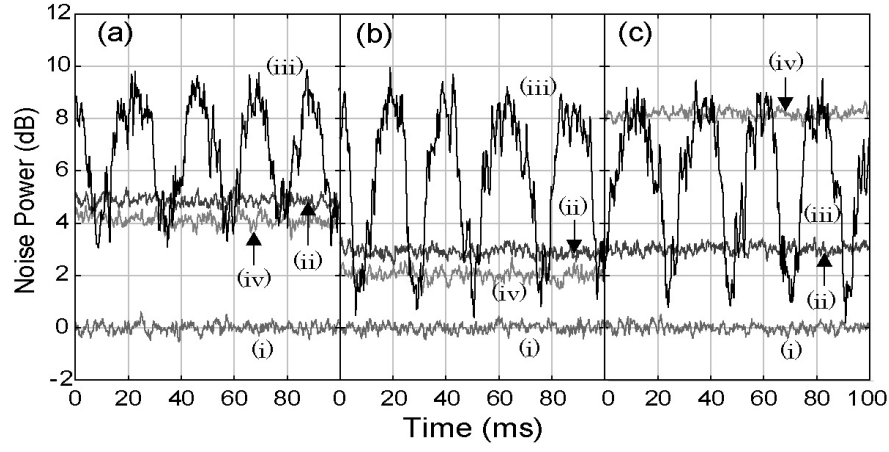


FIG. 4: Noise measurement results on the output states recorded by Victor's homodyne detector. Trace (a) shows the results for classical teleportation, namely without the EPR beams, in  $\hat{x}$  quadrature ( $\hat{p}$  quadrature is not shown). Traces (b) and (c) show the results for the teleportation with the EPR beams in  $\hat{x}$  and  $\hat{p}$  quadratures, respectively. In all cases, traces (i) represent the corresponding shot noise levels; traces (ii) are the variances for the vacuum state input; traces (iii) show the variances for the squeezed state input with the phase of the input state scanned. The Victor's LO phase is properly locked in  $\hat{x}$  or  $\hat{p}$  quadrature. Trace (iv) in (a) and trace (iv) in (b) are the minimum noise levels and trace (iv) in (c) is the maximum noise level with the phase of the input state locked. The measurement conditions are the same as for Fig 2.

measurement result on the input state shown in Fig 2. The inferred fidelity is  $0.734 \pm 0.04$  and we regard this value as the classical limit for the input. The measured fidelity of the classical case without the EPR beams is  $0.727 \pm 0.05$ , which is in good agreement with the classical limit. On the other hand, with the EPR beams, we obtain the result of  $F = 0.85 \pm 0.05$  which is higher than the classical limit. This fact shows the success of quantum teleportation and it means that the teleported state in the quantum teleportation is more close to the input state than that in the classical teleportation.

Note that the observed squeezed variance of the teleported state is larger than Victor's shot noise level, which shows that the output state is not a nonclassical state. More EPR correlation is required to get a nonclassical state at Bob's place. It is a next challenge to generate a teleported state whose variance is below the shot noise level.

In conclusion, we have demonstrated continuous variable quantum teleportation of a squeezed state. We observed the less variance of the teleported squeezed state than that for the case of the vacuum state input. It means that the nonclassical feature is preserved during the teleportation process. The measured fidelity of the squeezed state input in the quantum teleportation is  $0.85 \pm 0.05$  which is higher than the classical case  $0.73 \pm 0.05$ . This result shows that the teleported state in the quantum teleportation process is more similar to the input state than that in the classical teleportation. This work is an important step toward entanglement swapping.

This work was supported by the MEXT and the MHPPT of Japan, and Research Foundation for Opto-Science and Technology. We would like to thank Daniel Browne, Mio Muraio, Samuel Braunstein and Masahide Sasaki for valuable comments and discussions.

- 
- [1] C. H. Bennett et al, Phys. Rev. Lett. 70, 1895 (1993).
  - [2] M. A. Nielsen and I. L. Chuang, Quantum Computation and Quantum Information (Cambridge University Press, Cambridge, 2000).
  - [3] D. Bouwmeester et al, Nature (London) 390, 575 (1997).
  - [4] I. Marcikic et al, Nature (London) 421, 509 (2003).
  - [5] L. Vaidman, Phys. Rev. A 49, 1473 (1994).
  - [6] S. L. Braunstein and H. J. Kimble, Phys. Rev. Lett. 80, 869 (1998).
  - [7] A. Einstein, B. Podolsky, and N. Rosen Phys. Rev. 47, 777 (1935).
  - [8] A. Furusawa et al, Science 282, 706 (1998).
  - [9] W. P. Bowen et al, Phys. Rev. A 67, 032302 (2003).
  - [10] T. C. Zhang et al, Phys. Rev. A 67, 033802 (2003).
  - [11] M. Zukowski et al, Phys. Rev. Lett. 71, 4287 (1993).
  - [12] D. F. Walls and G. J. Milburn, Quantum Optics (Springer, Berlin, 1994).
  - [13] S. J. van Enk, Phys. Rev. A 60, 5095 (1999).
  - [14] H. F. Hofmann et al, Phys. Rev. A 62, 062304 (2000).
  - [15] R. Jozsa, J. Mod. Opt. 41, 2315 (1994).
  - [16] L.-M. Duan et al, Phys. Rev. Lett. 84, 2722 (2000).
  - [17] S. L. Braunstein, C. A. Fuchs, and H. J. Kimble, J. Mod. Opt. 47, 267 (2000).
  - [18] S. L. Braunstein et al, Phys. Rev. A 64, 022321 (2001).
  - [19] M. Ban, M. Sasaki, and M. Takeoka, J. Phys. A: Math. Gen. 35, L401 (2002).

[20] J. Twamley, J. Phys. A :M ath. G en. 29, 3723 (1996).